Voltage Quality Comparison of Space Vector PWM Voltage Source Multilevel Inverter under Symmetric and Nonsymmetric Switching Sequence Variants: Voltage Waveforms, Spectra and THD

Lopatkin N.N.
Mathematics, physics and informatics department
The Shukshin Altai State Humanities Pedagogical University (ASHPU)
Biysk, Russia
nikolay_lopatkin@mail.ru

***Abstract*—The paper offers the simple voltage source multilevel inverter space vector PWM algorithm (based on the oblique-angled coordinates of two delta voltages) with the optimum three-segment non-symmetric vectors switching sequence variant providing the instantaneous output voltage quarter-wave symmetry. The comparisons with the five-segment variant by the voltage waveforms, spectra and THD are performed under the same lowest frequency modulation index values. The offered three-segment variant advantages in the THD values and in the switching quantity per the output voltage cycle are shown via the PSIM simulation. The Mathcad-drawn executed space vector loci are also shown and the voltage THD is presented as the function of the amplitude modulation index.**

Keywords—multilevel inverter; voltage space vector PWM (SVPWM); oblique-angled coordinates; integer and fractional parts of delta voltages relative values; three-segment vectors switching sequence; quarter-wave symmetry; THD

I. INTRODUCTION

There are plenty of foreign publications that have been devoted to both circuitry and control of the multilevel voltage source inverters (MLVSI) or have included the special sections to consider them. Some new circuitry and control solutions make it possible not only to improve the MLVSI output voltage quality or output capability, but also to reduce losses in switches, or to use more cheap components. In addition to the classical monograph on pulse width modulation inverter control [1], the most significant releases for last years are the books [2-8] and the papers [9-12]. Also attention should be paid to the domestic review papers, in particular [13] and recent [14].

The continuous inexhaustible flow of publications on space vector (SV) PWM (SVPWM) in MLVSI makes us realize that the current algorithms versions are not the final ones, and further development and more improvements still are possible. One of the attractive approaches is the simplification of the basic calculations in SVPWM algorithms in MLVSI by using the oblique-angled coordinates of two delta voltages [15-20].

II. PROBLEM DEFINITION

The papers [15, 16] are devoted to the occurrence and the kinds of the oblique-angled coordinates. The paper [17] describes the possible barycentric and affine space vector coordinates on triangles, underlines the role of the integer and fractional parts of the delta voltages relative values as the coordinates and the duty cycles of the three nearest vectors, and offers the several two-coordinate and three-coordinate effective algorithms for finding the coordinates and the duty cycles of the being executed vectors. The new symmetric and easy calculated triangle type identifier is presented in [17, 18]. At last, the enough fast resource saving algorithm implementation on the base of the nonconventional five-segment switching sequence scheme is offered in [18-20].

The main used in [18-20] delta voltage formation principle is:

$$u^*_{kEXExy}(t_c) = \lfloor u^*_{ksREFxy} \rfloor + f_{kEXExy}(t_c), \quad (1)$$

here $u^*_{kEXExy}(t_c)$ is the relative value (in relation to the input direct voltage of the unit level U_d) of the instantaneous output delta voltage u_{xy} that is being executed during the current time t_c from the start of the clock cycle with number k, $k = 1 \ldots m_f$, m_f is the frequency modulation index, $m_f = f_c / f$, f_c and f are, respectively, clock and modulating frequencies; $u^*_{ksREFxy}$ is the relative value of the instantaneous reference delta voltage u_{REFxy} sampled for the midpoint of the k-th clock cycle,

$$u^*_{ksREFab} = m_a \sin\left((2\pi k - \pi)/m_f + 2\pi/3\right),$$
$$u^*_{kSREFbc} = m_a \sin\left((2\pi k - \pi)/m_f\right), \quad (2)$$

the amplitude modulation index is defined as follows:

$$m_a = \sqrt{3} \cdot U / U_d = \sqrt{3} \cdot U^* = U^*_{\Delta m}, \quad (3)$$

here U and U^* are the value and the relative value of the space vector magnitude, respectively, $U^*_{\Delta m}$ is the amplitude relative value of the reference delta voltages, $\lfloor x \rfloor$ means the rounding down x to the closest integer number, taking into account the sign (the "floor" function); $f_{kEXExy}(t_c)$ is the function, which is being executed during the current time t_c from the start of the clock cycle with number k, and it can possess only the values 0 and 1; the clock cycle mean value $\bar{f}_{kEXExy}$ of this function should correspond to the fractional part of the relative value of the instantaneous reference delta voltage u_{REFxy}:

$$\bar{f}_{kEXExy} = \{u^*_{ksREFxy}\}, \quad (4)$$

$\{x\}$ means the fractional part of x.

Fig. 1 shows the rhombus that is formed by the four nearest to the reference vectors, three of them are being used with the specified duty cycles over the clock cycle.

Unfortunately, despite the quite high output power quality described in [18-20], the used five-segment vectors switching sequence is not optimal from the point of view of the quantity of the switching per output voltage cycle. This sequence is oriented to the delta voltage formation, and it is not the same that is used in [1, 2] (the conventional variant).

The alternative vectors switching sequence variant is needed to be the competitor of not only variant of [18-20], but also of the conventional variant.

III. New Nonsymmetric Switching Sequence

The excellent MLVSI switching sequence solution is the applying the nonsymmetrical three-segment variant of the vectors switching sequence used in [18-20].

The main traces of the executed voltage space vector (EVSV) in the context of (u^*_{ab}, u^*_{bc}) coordinates are shown in Fig. 2 for the first three rings of triangles. Here dashed lines correspond to the EVSV auxiliary transitions, namely transitions to the initial triangle vector after next sample inside the same triangle or, sometimes, to the transitions between the non-neighbor triangles.

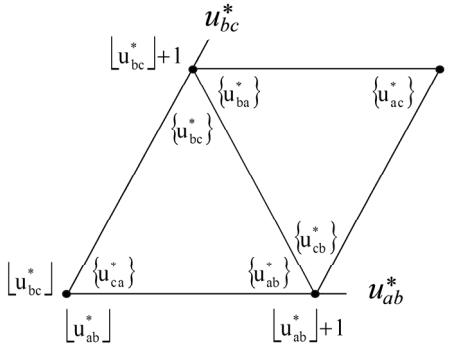

Fig. 1. The integer and the fractional parts of the reference delta voltages relative values as the coordinates and the duty cycles of the three nearest vectors over the clock cycle.

The set (in ascending order of the sector number) of the sequences of the being executed vectors inside the triangles for the first ring of modulating triangles is {(1,0),(0,0),(0,1); (0,1),(0,0),(-1,1); (-1,1),(0,0),(-1,0); (-1,0),(0,0),(0,-1); (0,-1),(0,0),(1,-1); (1,-1),(0,0),(1,0)}. With the appearance of the down pointed triangle in the second ring of modulating triangles, the moving of the EVSV endpoint has performed along the zigzag line. So, the set of the vector sequences in sector I of the second ring is {(2,0),(1,0),(1,1); (1,0),(1,1),(0,1); (1,1),(0,1),(0,2)}. The same order is kept at every transition to the subsequent sector. Therefore, the set of the vector sequences in sector II of the second ring is {(0,2),(0,1),(-1,2); (0,1),(-1,2),(-1,1); (-1,2),(-1,1),(-2,2)}, and so on.

As can be seen, every transition to the next ring adds two triangles (one triangle of each type) per sector, keeping both the EVSV trajectory of the moving inside the triangle of each type and the type of the initial (and the final) triangle in each sector.

The information, concerning the fractional component functions of (9), $f_{kxy}(t_c)$, is generalized by means of the consideration of this rhombus and presented in Table I.

The delta voltages behaviors in the reference SV moving process has been analyzed, and the pulses positions of the fractional component functions in (1), $f_{kEXExy}(t_c)$, are generalized by means of the consideration of the rhombus in Fig. 1 and have been completely defined as functions of the only two sampled reference delta voltages.

The fractional component function $f_{EXEab}(t_c)$ of the executed delta voltage $u^*_{kEXEab}(t_c)$ is presented in Table I. The fractional component function $f_{EXEbc}(t_c)$ may be also obtained by $2\pi/3$ phase shift of the function $f_{EXEab}(t_c)$ (their similarity can be seen in [18]).

The Table I makes it possible to use the triangular carrier voltages and few modulating signals composed of the fractional components of the two reference delta voltages sampled relative values, sector identifier and one of the triangle type identifiers [17, 18].

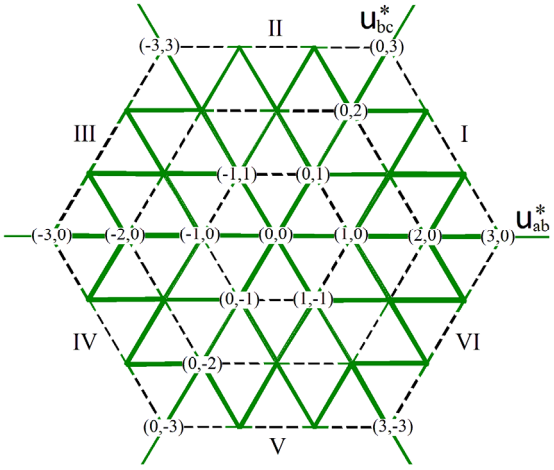

Fig. 2. The main traces of the executed voltage space vector under offered switching sequence.

TABLE I. FRACTIONAL COMPONENT FUNCTION

Sector	Triangle Type and EVSV Trajectory	Fractional Component Function of Executed Delta Voltage $f_{EXEab}(t_c)$
I 0°…60°	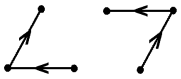	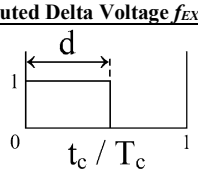 $d = \{u^*_{ab}\}$
II 60°…120°		
III 120°…180°		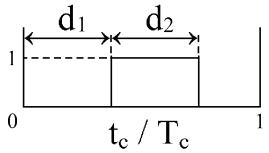 $d_1 = \{u^*_{bc}\}$ $d_2 = \{u^*_{ab}\}$
		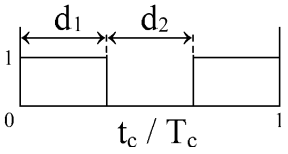 $d_1 = \{u^*_{ab}\} + \{u^*_{bc}\} - 1$ $d_2 = 1 - \{u^*_{ab}\}$
IV 180°…240°	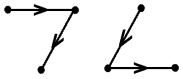	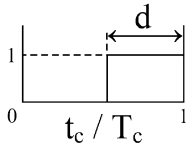 $d = \{u^*_{ab}\}$
V 240°…300°		
VI 300°…360°		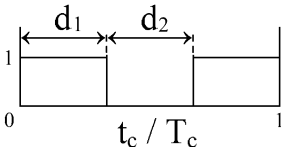 $d_1 = 1 - \{u^*_{bc}\}$ $d_2 = 1 - \{u^*_{ab}\}$
		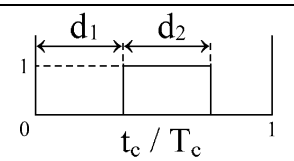 $d_1 = 1 - \{u^*_{ab}\} - \{u^*_{bc}\}$ $d_2 = \{u^*_{ab}\}$

IV. SIMULATION RESULTS

A. Voltages Waveforms, Spectra and Space Vector Loci Simulation

It is generally accepted that the frequency modulation index must be divisible both by 2 (the number of the half-waves) and by 3 (the number of the MLVSI phases), i.e. it must be divisible by 6. So, the lowest studied values of the frequency modulation index are $m_f = 12$ and $m_f = 18$.

The PSIM-simulated idealized waveforms of the output delta voltage u^*_{EXEbc}, the phase-to-neutral voltage u^*_{EXEbn} and the phase-to-ground voltage u^*_{EXEbg}, as well as the delta voltage spectrum and the Mathcad-simulated executed space vector locus are presented for $m_f = 12$ at $m_a = 0.5$, $m_f = 12$ at $m_a = 3.5$, and $m_f = 18$ at $m_a = 3.5$ in Fig. 3…Fig. 8 for the before used [18-20] symmetric five-segment variant and the new offered nonsymmetric three-segment variant of the vectors switching sequence.

The phase-to-neutral executed voltages correspond to the well known matrix equation:

$$\begin{bmatrix} u^*_{EXEan} \\ u^*_{EXEbn} \\ u^*_{EXEcn} \end{bmatrix} = \frac{1}{3} \cdot \begin{bmatrix} 2 & 1 \\ -1 & 1 \\ -1 & -2 \end{bmatrix} \cdot \begin{bmatrix} u^*_{EXEab} \\ u^*_{EXEbc} \end{bmatrix}, \tag{5}$$

and the directly executed phase-to-ground voltages have been chosen here as having the minimum instantaneous values [16]:

$$u^*_{EXEag} = \max\left(0, u^*_{EXEab}, u^*_{EXEab} + u^*_{EXEbc}\right), \tag{6}$$

$$u^*_{EXEbg} = u^*_{EXEag} - u^*_{EXEab} = \max\left(-u^*_{EXEab}, 0, u^*_{EXEbc}\right),$$

$$u^*_{EXEcg} = u^*_{EXEbg} - u^*_{EXEbc} = \max\left(-u^*_{EXEab} - u^*_{EXEbc}, -u^*_{EXEbc}, 0\right).$$

The spectral diagrams show the amplitude ratios of the n-th order and the fundamental harmonics of the output delta voltage.

The blue arrows in the space vector loci diagrams show the transitions between the sequentially executed space vectors. Enough high values of m_a at enough low values of m_f produce some loopless degenerate kind of the EVSV trajectory for the offered three-segment switching sequence (the reference SV doesn't fall twice into the modulating triangles, see Fig. 6 and Fig. 8).

The considered symmetric five-segment and the new offered nonsymmetric three-segment switching sequence variants comparison shows the following features:

a) the presence of the same orders harmonics at any values of the frequency modulation and the amplitude modulation indices for the both vectors switching sequence variants, namely harmonics with numbers $n = 6 \cdot k \pm 1$, here k belongs to the natural numbers;

b) unlike the five-segment variant with the only half-wave symmetry of the instantaneous both delta and phase-to-neutral voltages waveforms, that means $u(\omega t) = -u(\omega t + \pi)$ and leads to the absence of the even-order harmonics, the three-segment

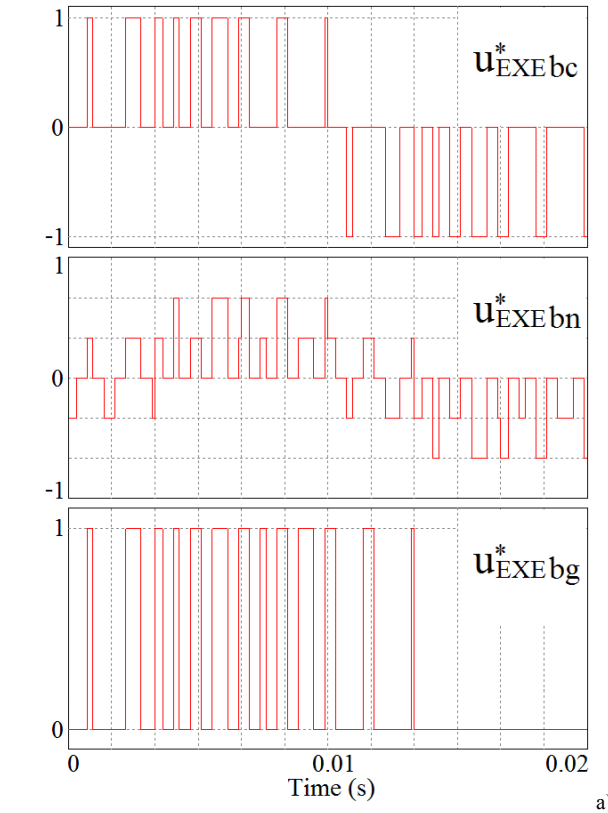

a)

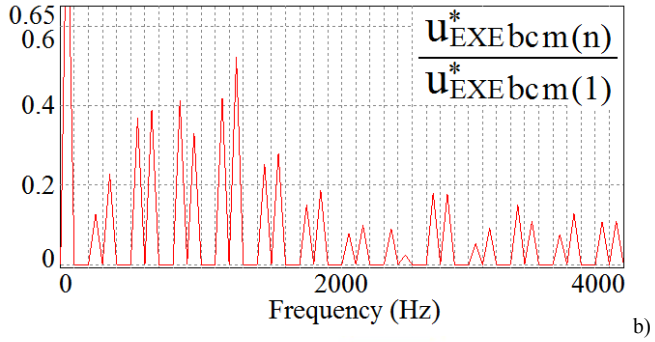

b)

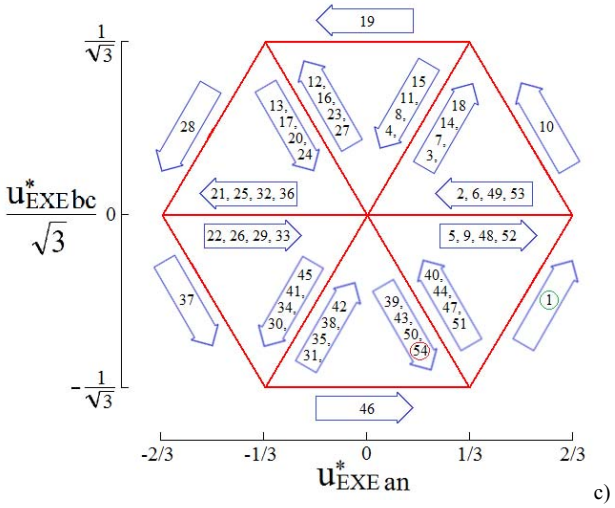

c)

Fig. 3. The simulation results for the five-segment vectors switching sequence under m_f = 12 and m_a = 0.5: a) waveforms of output delta, phase-to-neutral and phase-to-ground voltages; b) delta voltage spectrum; c) executed space vector locus.

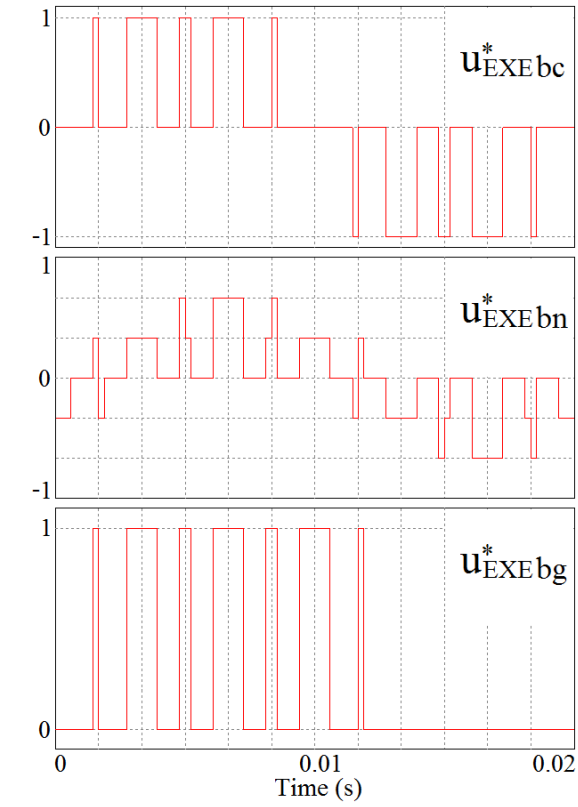

a)

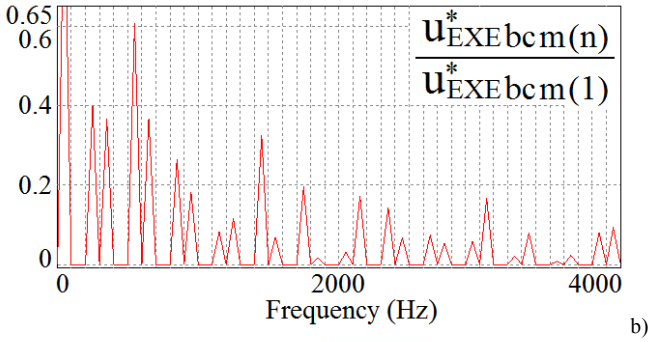

b)

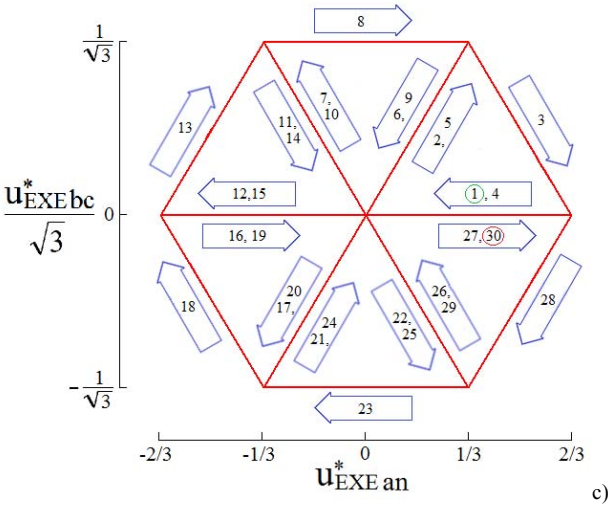

c)

Fig. 4. The simulation results for the three-segment vectors switching sequence under m_f = 12 and m_a = 0.5: a) waveforms of output delta, phase-to-neutral and phase-to-ground voltages; b) delta voltage spectrum; c) executed space vector locus.

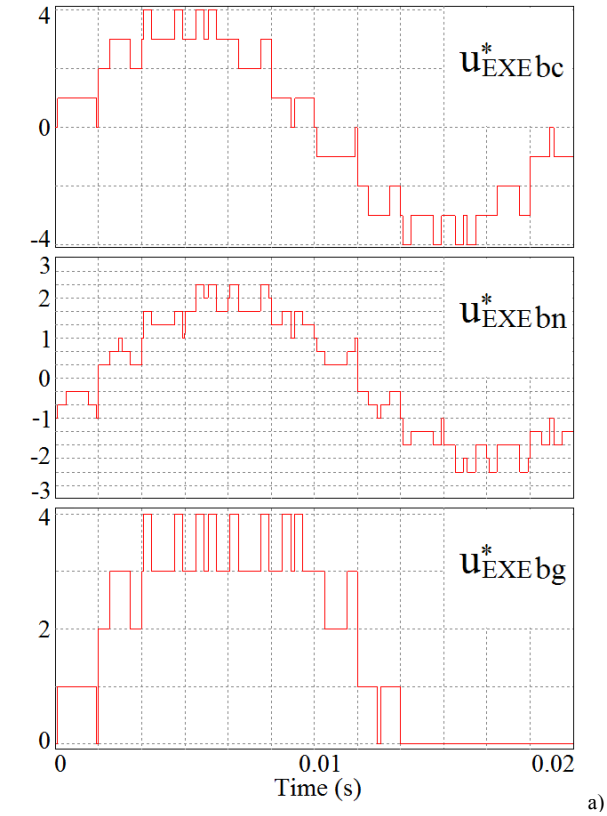

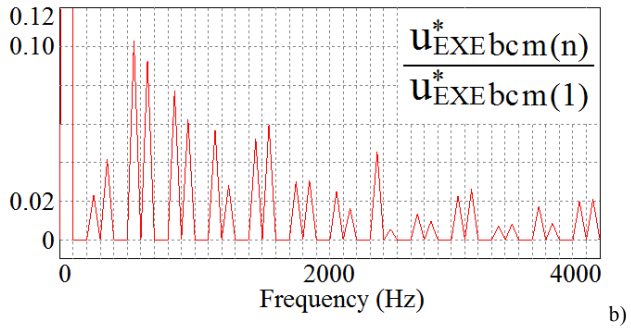

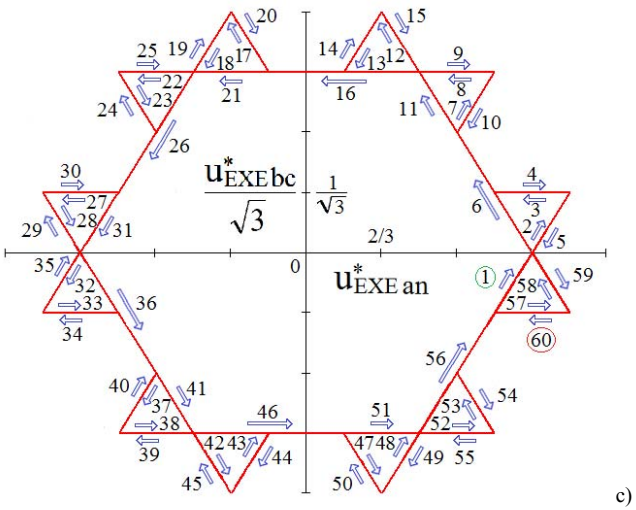

Fig. 5. The simulation results for the five-segment vectors switching sequence under m_f = 12 and m_a = 3.5: a) waveforms of output delta, phase-to-neutral and phase-to-ground voltages; b) delta voltage spectrum; c) executed space vector locus.

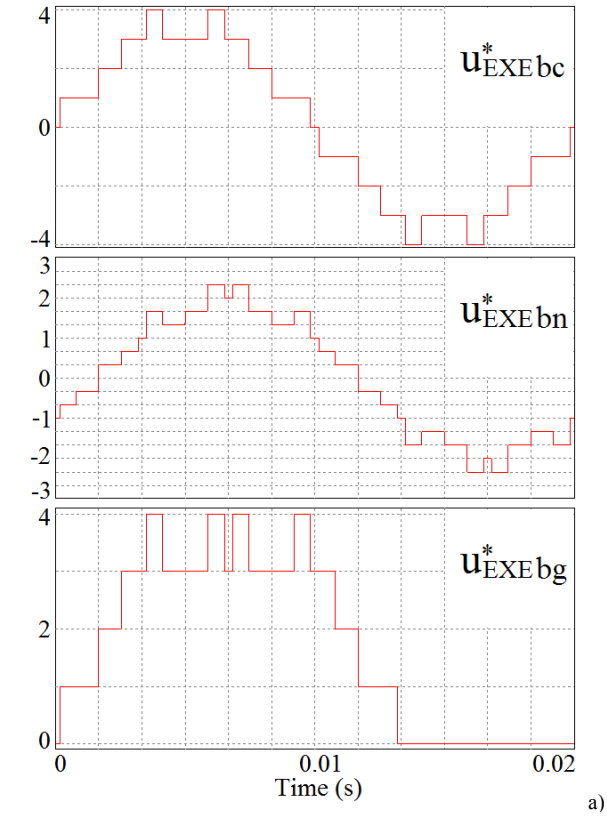

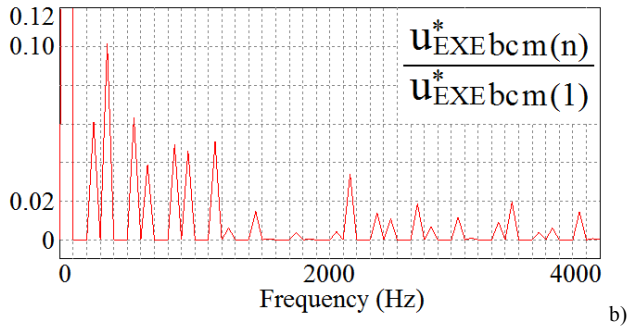

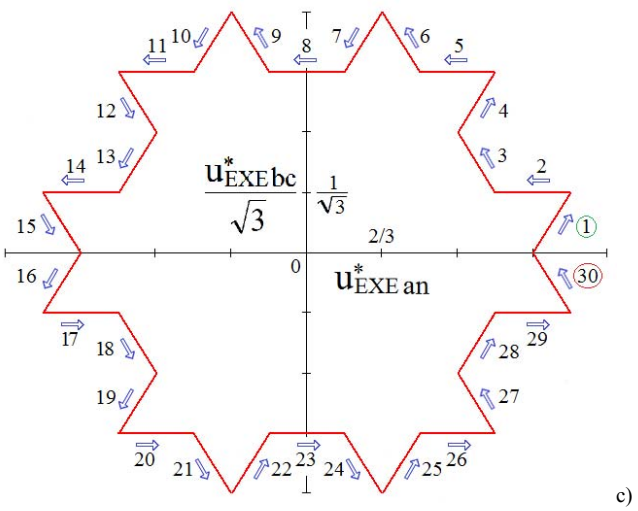

Fig. 6. The simulation results for the three-segment vectors switching sequence under m_f = 12 and m_a = 3.5: a) waveforms of output delta, phase-to-neutral and phase-to-ground voltages; b) delta voltage spectrum; c) executed space vector locus.

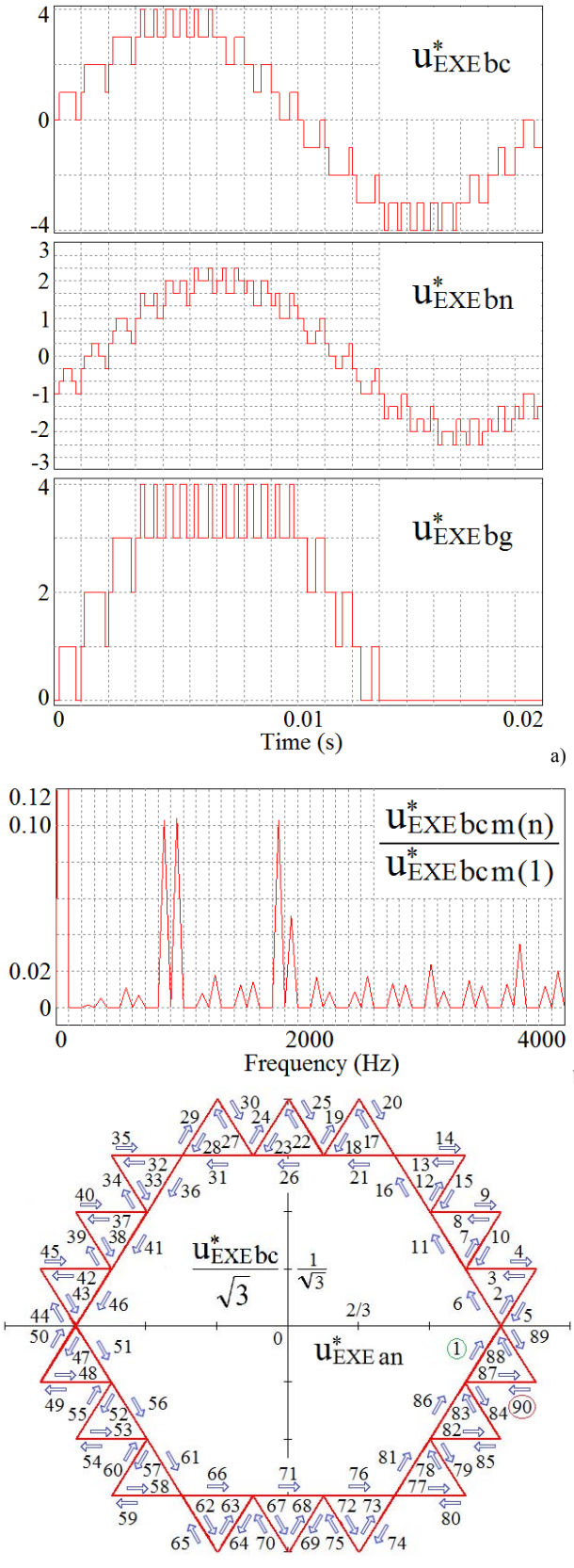

Fig. 7. The simulation results for the five-segment vectors switching sequence under m_f = 18 and m_a = 3.5: a) waveforms of output delta, phase-to-neutral and phase-to-ground voltages; b) delta voltage spectrum; c) executed space vector locus.

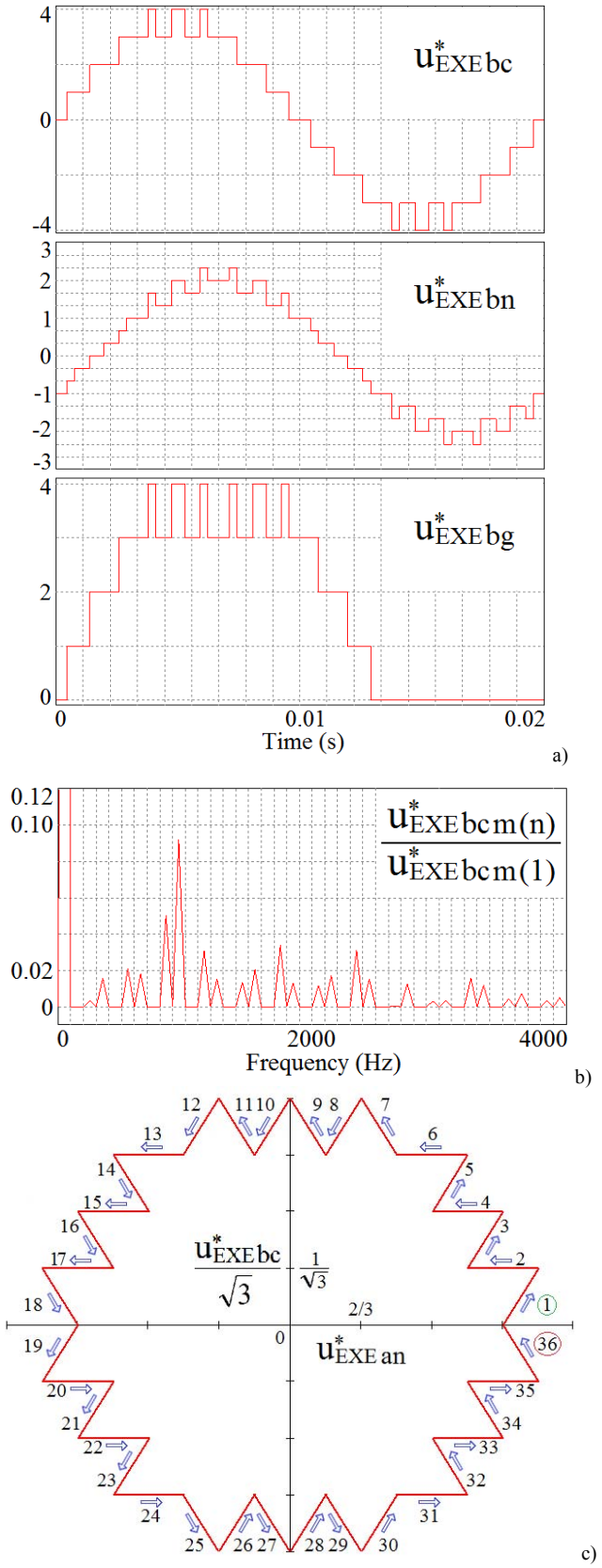

Fig. 8. The simulation results for the three-segment vectors switching sequence under m_f = 18 and m_a = 3.5: a) waveforms of output delta, phase-to-neutral and phase-to-ground voltages; b) delta voltage spectrum; c) executed space vector locus.

variant also provide the quarter-wave symmetry for these voltages waveforms, i.e. $u(\omega t) = u(-\omega t)$ or $-u(\omega t) = u(-\omega t)$ can be added under the appropriate choice of the zero-time reference, leading to the absence of the sine or the cosine components in the remaining harmonics, respectively;
c) unlike the five-segment variant, the three-segment one never has transitions with the delta voltage changes that exceed one base level;
d) both the phase-to-ground voltages waveforms and the loci diagrams demonstrate the three-segment variant advantage in switchings number at the comparable harmonic content level.

It must be noted that none of the conventional clock cycle symmetric pulse patterns of SVPWM leads to the quarter-wave symmetric waveform of the output voltage. The new algorithm in [12] is providing this kind of the symmetry due to the modulation index segmentation and the designing the switching sequences specially for each segment. Despite the algorithm is really very interesting and thoroughly developed, it has a high degree of complexity and so it is limited now by the three level inverter.

B. Delta Voltage THD Mathcad Simulation

To obtain the continuous curves of the dependences of the output voltage THD on the amplitude modulation index, the Mathcad model was built, and the waveform Fourier coefficients for every of the m_f clock cycle intervals were defined.

The three-segment sequence versus the five-segment sequence simulation graphs of the MLVSI output delta voltage THD dependences on the amplitude modulation index are presented for $m_f = 12$, $m_f = 18$ in Fig. 9 a, and for $m_f = 24$, $m_f = 30$ in Fig. 9 b, respectively. Fig. 10 presents the same dependences for the only three-segment vectors switching sequence under the five lowest values of the frequency modulation index: $m_f = 12$, 18, 24, 30, and 36.

The direct THD values comparisons for the considered symmetric five-segment and the new offered nonsymmetric three-segment vectors switching sequence variants in Fig. 9 show that the offered three-segment variant has the clear superiority. Moreover, the THD values of the 3-segment variant at $m_f = 24$ are always less than the values of the 5-segment variant at $m_f = 30$, and similarly the THD values of the 3-segment variant at $m_f = 12$ are almost always less than the values of the 5-segment variant at $m_f = 18$.

Nevertheless, we shouldn't make some far-reaching conclusions about the output energy quality advantage of one of the studied switching sequence variants without the output (load) current THD consideration. But the current THD value doesn't directly depend on the corresponding voltage THD value, and it depends on the various order integral factors of voltage harmonics (IFH). The offered by the professor G.S. Zinoviev (NSTU, Novosibirsk) IFH include the load filtering effect on the investigated voltage signal [21, 22]. Their comparison for the two studied switching sequence variants is the subject of the separate paper.

The consideration of the curves in Fig. 10 displays the two facts. Firstly, the more the value of the frequency modulation index m_f is, the closer corresponding adjacent to each other curves are situated. Secondly, the more the value of the frequency modulation index m_f is, the more the value of the amplitude modulation index m_a which provides the THD value less than previous frequency modulation index value produces.

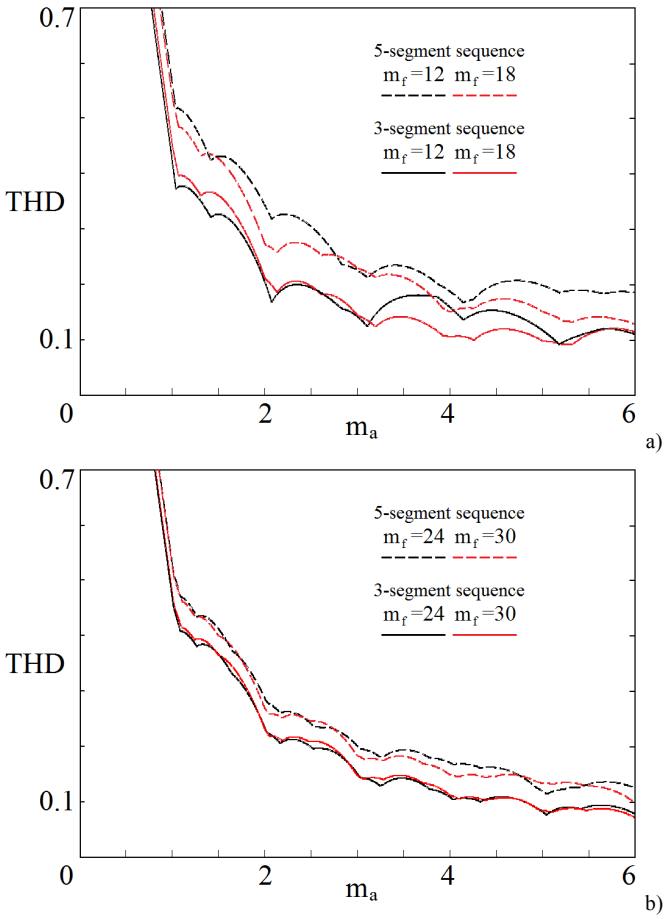

Fig. 9. The Mathcad THD simulation results for the five-segment and the three-segment switching sequences: a) under $m_f = 12$ and $m_f = 18$; b) under $m_f = 24$ and $m_f = 30$.

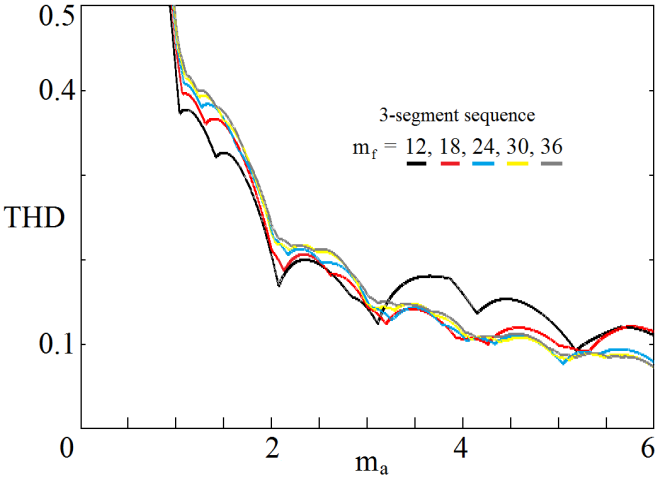

Fig. 10. The Mathcad THD simulation results for the offered three-segment switching sequence under the five lowest values of the frequency modulation index.

V. CONCLUSIONS

The new three-segment nonsymmetric vectors switching sequence variant providing the instantaneous output voltage quarter-wave symmetry is offered for the simple delta voltages space vector PWM algorithm applied to any arbitrary circuit of the voltage source multilevel inverter with any arbitrary number of the equal feeding DC voltage levels. This algorithm has been beforehand developed for oblique-angled coordinates of two delta voltages on the base of one of the more general algorithms. The implementation of the offered algorithm key steps is shown for the new offered three-segment switching sequence variant.

The PSIM-simulated idealized waveforms of the output delta voltage, the phase-to-neutral voltage and the phase-to-ground voltage, as well as the delta voltage spectrum and the Mathcad-simulated executed space vector locus are presented for the before used symmetric five-segment variant and the new offered nonsymmetric three-segment variant of the vectors switching sequence at the low values of the frequency modulation index. Due to the development of the spectral Mathcad model, the voltage THD dependences on the amplitude modulation index are obtained.

As the result of the switching sequence variants comparison the advantages of the new offered nonsymmetric three-segment variant in both the switchings number per output voltage cycle and the THD values are revealed for the entire range of the amplitude modulation index values.

However, the supplementary investigation is needed to estimate the integral factors of voltage harmonics, which are defining the load current quality, in particular its THD value.

REFERENCES

[1] D.G. Holms, T.A. Lipo, Pulse Width Modulation for Power Converters, Piscataway, NJ: IEEE Press, 2003.

[2] Bin Wu, High-Power Converters and AC Drives, Wiley-IEEE Press, 2006.

[3] Bin Wu, M. Narimani, High-Power Converters and AC Drives, Wiley-IEEE Press, 2017.

[4] S.A. Gonzalez, S.A. Verne, M.I. Valla, Multilevel Converters for Industrial Applications, CRC Press, 2013.

[5] F.L. Luo, H.Ye, Advanced DC/AC Inverters: Applications in Renewable Energy, CRC Press, 2013.

[6] B. Ge, F.Z. Peng, and Y. Li, "Multilevel Converter/Inverter Topologies and Applications," Chapter 14 in Power Electronics for Renewable Energy Systems, Transportation and Industrial Applications, pp. 422-462, 2014.

[7] S. Stynski, M. Malinowski, "Space Vector Modulation in Three-Phase Three-Level Flying Capacitor Converter-Fed Adjustable Speed Drive," Chapter 10 in Advanced and Intelligent Control in Power Electronics and Drives, pp. 335-374, 2014.

[8] E.C. dos Santos, E.R.C. da Silva, Advanced Power Electronics Converters: PWM Converters Processing AC Voltages, Wiley-IEEE Press, 2015.

[9] S. Kouro, M. Malinowski, K. Gopakumar, J. Pou, L.G. Franquelo, Bin Wu, J. Rodriguez, M.A. Pérez, and J.I. Leon, "Recent advances and industrial applications of multilevel converters," IEEE Transactions on Industrial Electronics, vol. 57, is. 8, pp. 2553-2580, 2010.

[10] A.R. Beig, S. Kanukollu, K. Al Hosani, A. Dekka, "Space-vector-based synchronized three-level discontinuous PWM for medium-voltage high-power VSI," IEEE Transactions on Industrial Electronics, vol. 61, is. 8, pp. 3891-3901, 2014.

[11] J.I. Leon, S. Kouro, J. Rodriguez, Bin Wu, "The essential role and the continuous evolution of modulation techniques for voltage-source inverters in the past, present, and future power electronics," IEEE Transactions on Industrial Electronics, vol. 63, is. 5, pp. 2688-2701, 2016.

[12] W. Chen, H. Sun, X. Gu, and C. Xia, "Synchronized space vector PWM for three level VSI with lower harmonic distortion and switching frequency," IEEE Transactions on Power Electronics, vol. 31, is. 9, pp. 6428-6441, 2016.

[13] G.S. Zinoviev, N.N. Lopatkin, "Evolution of multilevel voltage source inverters," in Proc. Actual Problems of Electronic Instrument Engineering, APEIE, Novosibirsk, 2008, vol. 1, pp. 125-136.

[14] I.A. Bakhovtsev, G.S. Zinovev, "PWM methods evolution," in Proc. Actual Problems of Electronic Instrument Engineering, APEIE, Novosibirsk, 2016, vol. 10, pp. 129-144.

[15] N. Celanovic, D. Boroyevich, "A fast space-vector modulation algorithm for multilevel three-phase converters," IEEE Transactions on Industry Applications, vol. 37, is. 2, pp. 637-641, 2001.

[16] N.N. Lopatkin, "Representation of the voltage space vector of the multilevel inverter in oblique-angled coordinate systems of two delta voltages," in Proc. Actual Problems of Electronic Instrument Engineering, APEIE, Novosibirsk, 2014, vol. 1, pp. 824-828.

[17] N.N. Lopatkin, "Some new representations of the multilevel inverter voltage space vector in the complex plane," in Proc. International Siberian Conference on Control and Communications, SIBCON, Russia, Omsk, 2015. Proceedings.

[18] N.N. Lopatkin, "Simple delta voltages space vector PWM algorithm for voltage source multilevel inverters," in Proc. Intelligent Energy and Power Systems, IEPS, Kyiv, Ukraine, 2016, pp. 149-154.

[19] N.N. Lopatkin, "Output voltage simulation of multilevel inverter with space vector modulation of two delta voltages," Technical Electrodynamics, is. 5, pp. 20-22, 2016.

[20] N.N. Lopatkin, "Voltage harmonics integral factors estimation of multilevel inverter with space vector modulation of two delta voltages," in Proc. Actual Problems of Electronic Instrument Engineering, APEIE, Novosibirsk, 2016, vol. 1, part 3, pp. 112-115.

[21] G.S. Zinoviev, Power Electronics. Textbook for undergraduate students, Moscow: Jurajt, 2012.

[22] N.N. Lopatkin, Y.A. Chernov, "Virtual instrument for nonconventional total harmonic distortion factors evaluation," in Proc. International Siberian Conference on Control and Communications (SIBCON), Russia, Moscow, 2016.